Washcoated Pd/Al_2O_3 monoliths for the liquid phase hydrodechlorination of dioxins

Martha Cobo[a,*], *Andrés* Orrego[b], and *Juan A.* Conesa[c]

[a]Energy, Materials and Environment Laboratory, Chemical Engineering Department, University of La Sabana, Campus Universitario Puente del Común, Km. 7 Autopista Norte, Bogotá (Colombia)

[b]Environmental Catalysis Laboratory, Sede Investigación Universitaria, University of Antioquia. Carrera 53 N°. 61-30, Medellín, Colombia.

[c]Department of Chemical Engineering, University of Alicante, P.O. Box 99, E-03080 Alicante, Spain.

*Corresponding author: Email: martha.cobo@unisabana.edu.co, Tel: +571 8615555 Ext. 2537, Fax: +571 8615555

Abstract

The catalytic activity and durability of 2 wt. % Pd/Al_2O_3 in powder and washcoated on cordierite monoliths were examined for the liquid phase hydrodechlorination (LPHDC) of polychlorinated dibenzo-p-dioxins/polychlorinated dibenzofurans (PCDD/Fs). NaOH was employed as a neutralizing agent, and 2-propanol was used as a hydrogen donor and a solvent. Fresh and spent powder and monolith samples were characterized by elemental analysis, surface area, hydrogen chemisorption, scanning electron microscopy/energy dispersive X-ray spectroscopy (SEM/EDX), and transmission electron microscopy/energy dispersive X-ray spectroscopy (TEM/EDS). Three reactor configurations were compared including the slurry and monolith batch reactors as well as the bubble loop column resulting in 100, 70, and 72% sample toxicity reduction, respectively, after 5 h of reaction. However, the slurry and monolith batch reactors lead to catalyst sample loss via a filtration process (slurry) and washcoat erosion (monolith batch), as well as rapid deactivation of the powder catalyst samples. The monolith employed in the bubble loop column remained stable and active after four reaction runs. Three preemptive regeneration methods were evaluated on spent monolith catalyst including 2-propanol washing, oxidation/reduction, and reduction. All three procedures reactivated the spent catalyst samples, but the combustion methods proved to be more efficient at eliminating the more stable poisons.

Keywords: Pd/Al_2O_3 catalyst, washcoated monoliths, catalyst deactivation, dioxins, fly ash.

1. Introduction

Catalytic hydrodechlorination (HDC) over noble metal supported catalysts is one of the most promising methods for the degradation of chlorinated wastes from gas and liquid phases (Keane, 2011). Among the noble metals, Pd exhibits high activity and poisoning resistance (Yuan, 2004, Cobo, 2011). Polychlorinated dibenzo-p-dioxins/polychlorinated dibenzofurans (PCDD/Fs), which are also known as dioxins, are a group of highly toxic compounds generated from a wide range of anthropogenic sources in the gas, liquid, and solid phases (Cobo, 2009a). Fly ash produced in solid waste incinerators contains one of the highest amounts of dioxin waste, and the extraction of the dioxins with organic solvents for further treatment has been recently investigated. Liquid phase hydrodechlorination (LPHDC) of dioxins over 2 wt. % Pd/γ-Al_2O_3 using 2-propanol as a hydrogen donor and solvent has been successfully accomplished in a slurry reactor under mild conditions (Ukisu, 2004, Cobo, 2009b). This reaction involves the interaction between the liquid phase where the organic compound is dissolved, the hydrogen gas phase, which is produced *in-situ* by 2-propanol decomposition, and the catalyst solid phase. Good mixing of the involved phases will reduce the mass and heat transfer limitations resulting in a proper heterogeneous catalytic reaction. This goal can be achieved either in slurry or in fixed bed reactors (Gómez-Quero, 2011). However, these configurations are affected by catalyst separation, reuse, presence of mass and heat transfer artifacts, pressure drop, and over costs in industrial scale implementation (Fishwck, 2007).

Although the most widely used catalytic systems for environmental applications with gas-phase reactions are monolithic materials (Avila, 2005), multiphase gas–liquid reactions using monolith catalysts have recently become of interest to the academic and industrial community. The first large-scale application was the production of hydrogen peroxide via the anthraquinone process

developed by Akzo Nobel, which illustrated the potential for monolith reactors to replace other conventional reactor types in certain applications (Smiths, 1996, Albers, 2001, Albers, 2005). In addition, washcoated monoliths have been employed in reactor devices, such as the gradientless Berty reactor for the selective hydrogenation of benzaldehyde over Ni/Al_2O_3 (Xiaoding, 1996), the monolithic stirred reactor for styrene hydrogenation over Pd/SiO_2 (Nijhuis, 2003) and sunflower oil hydrogenation over Pd/Al_2O_3 (Sanchez, 2009), the monolith down flow bubble column for several hydrogenation reactions (Cybulski , 1999, Nijnuis, 2001, 2003, Marwan, 2004), the monolith loop configuration for mass transfer simulations (Heiszwolf, 2001, Vandu, 2005) and glucose hydrogenation over Rh/Al_2O_3 (Eisenbeis, 2009), and the monolith cocurrent downflow contactor (CDC) for the hydrogenation of 2-butyne-1,4-diol over Pd/Al_2O_3 (Kulkarni, 2005, Fishwck, 2007). A comparison of monolithic and traditional fixed bed reactors has shown that monoliths afford superior performance, such as low pressure drop, high geometric surface area, high resistance to blockage, high selectivity, high volumetric productivity for a smaller amount of catalyst, elimination of the filtration step, high mass transfer rates, and easier scale-up (Fishwick, 2007, Tsoligkas, 2007, Moulijn, 2011). In addition, monoliths have become important in photocatalysis (Morales, 2001, Yu, 2011), biotechnology (Ebrahimi, 2006, Delattre, 2009), and liquid-phase chromatography (Huang, 2012). The optimization of the reactor configuration is a dynamic issue, especially when looking for good multiphase interactions. To the best of our knowledge, there are no previous reports using monolith reactors for the liquid phase hydrodechlorination of chlorinated wastes.

In this paper, we report the catalytic performance of 2 wt. % Pd/Al_2O_3 washcoated cordierite monoliths for the LPHDC of dioxins, and the performance of a slurry reactor, monolith batch reactor, and bubble loop column are compared. The monolith catalysts were tested for washcoat stability and characterized by elemental analysis, BET surface area, hydrogen chemisorption,

SEM/EDS, and TEM/EDS. In addition, the durability and regeneration of the 2 wt. % Pd/Al_2O_3 washcoated monolith samples were examined.

2. Materials and methods

2.1. Catalyst preparation

The powder catalyst samples employed in the slurry reactor were prepared by dissolving the required amount of palladium acetylacetonate (99%, Aldrich Chem. Co., USA) in acetone, which was added to a given amount of γ-alumina support (99.97%, Alfa Aesar, USA) to obtain a 2 wt. % Pd loading. The mixture was magnetically stirred for 24 h. Then acetone was rotavapored, and the solid calcined with a heating rate of 2 °C/min up to 400 °C for 2 h in 50 mL/min flowing air, reduced in 50 mL/min flowing 10% H_2/N_2, and heated at 2 °C/min to 300 °C.

Square cordierite monoliths (Corning Inc., New York, USA) with 400 cpsi (cells per square inch), 0.18 mm average wall thickness, 6 x 6 frontal channels (7.2 cm x 7.2 cm), and 1.2 cm long were employed. Cordierite monoliths were washcoated according to a previously published protocol (Gonzalez et al., 2007). In this procedure, the monolith samples were treated in 20 % w/w HNO_3 solution for 3 h and water washed until neutral. Then they were oven dried at 100 °C for 24 h, aged in acetone for 24 h, and calcined in static air with a heating rate of 2 °C/min up to 600 °C for 2 h. The washcoat slurry was prepared as follows: powder 2 wt. % Pd/Al_2O_3 was slurred into water to obtain 25 wt. % solids and 5 wt. % alumina sol binder (pseudoboehmite) to improve the binding strength (Avila, 2005, Gonzalez, 2007). The slurry was ball-milled at 90 rpm for 24 h. The resulting slurry, which had a pH of 7 and 23 wt. % solids, was employed for monolith washcoating via the dip-coating method (Marwan, 2007). The outer monolith faces were covered such that the

depositions only occurred inside the channels (Zamaro, 2005a, 2005b). The washcoating was performed according to a previously published protocol as follows (Gonzalez, 2007): (1) The monoliths were dipped into a 2 wt. % Pd/Al_2O_3 water slurry (23 wt. % solids) for 10 s. (2) The excess slurry was softly blown off with compressed air (7.4 MPa) keeping the monoliths in a vertical position for 10 s and avoiding shaking the monolith to maintain washcoat uniformity. (3) The samples were dried in a microwave oven for 6 min to obtain a uniform Pd distribution, and then weighed. Steps 1-3 were repeated until a 100 mg of washcoat was achieved. (4) Then the washcoated monoliths were calcined in air with a heating rate of 2 ºC/min from room temperature to 400 ºC for 2 h in 50 mL/min flowing air, reduced in 50 mL/min flowing 10% H_2/N_2, and heated at 2 °C/min to 300 °C

The monolith washcoat adhesion and abrasion were assessed through different resistant tests (Gonzalez, 2007). The monolith samples were subjected to ultrasonic vibration in either aqueous or 2-propanol media for 1 h in a Branson 3510 ultrasonic vibration cleaner (Emerson Electric Co., GA, USA). Then, the samples were dried, weighed, and subjected to aging. These tests were performed in quadruplicate. In addition, 70 mL/s water flow was passed through the monolith for approximately 30 min, dried and weighed to determine the flow effects on washcoat abrasion. Finally, the monolith was tested under simulated reaction conditions in 2-propanol for 6 h at reaction temperature (75 °C), dried and weighed. The decrease in monolith washcoat weight after each test was taken as a measure of washcoat resistance (Gonzalez, 2007, Zamaro, 2005b).

2.2 Catalyst characterization

The fresh and spent samples of the powder and monolith samples of 2 wt. % Pd/Al_2O_3 were characterized by various techniques. The elemental analysis was performed by atomic absorption in

a Philips PU9200 apparatus (Philips, The Netherlands). Single point Brunauer-Emmet-Teller (BET) surface area and pulse chemisorption were performed with an AutoChem II 2920 Micromeritics instrument (USA) equipped with a thermal conductivity detector (TCD). Scanning electron microscopy (SEM) studies of the 2 wt. % Pd/Al_2O_3 washcoated monolith samples were performed with a JEOL-JSM 840 model equipped with an energy dispersive X-ray spectroscopy (EDX) analyzer (SEMTech Solutions, USA). Transmission electron microscopy (TEM) was performed with a JEOL JEM-2010 microscope (Japan) coupled to an energy dispersive X-ray spectroscopy (EDS system OXFORD instruments INCA Energy TEM100, UK). The samples were dispersed in ethanol by ultrasonic vibration and dropped on a copper grid coated with a carbon film. At least 200 individual Pd particles were counted for each catalyst sample, and the mean Pd particle size is reported as the surface-area-weighted average size ($\bar{d}Pd$) (Yuan, 2004, Cobo, 2009b).

2.3 Experimental set up

2.3.1 Slurry batch reactor tests

LPHDC reactions were performed in a slurry batch reactor as described in a previously published protocol (Cobo, 2008a, 2009b). Approximately 77.35 ng I-TEQ of PCDD/Fs fly ash extract and 100 mg of 2 wt. % $Pd/\gamma\text{-}Al_2O_3$ catalyst were added to 20 mL of 50 mM NaOH in a 2-propanol solution. The resulting mixture was magnetically stirred at 2300 rpm and maintained 75 °C (±1°C) for various time periods. After the reaction, the catalyst samples were recovered by filtration, washed with 100 mL of toluene, and dried at 100 °C for 24 h. The absence of mass transfer limitations was previously verified (Cobo, 2009b).

2.3.2 Monolithic reactor tests

The experimental setup to examine the reactivity of 2 wt. % Pd/Al_2O_3 washcoated monoliths in a bubble loop column is shown in Figure 1. A washcoated monolith containing approximately 100 mg of 2 wt. % Pd/Al_2O_3 was placed in a glass container (0.015 m I.D. and 0.15 m long), and the reaction mixture (the same as employed for the slurry reactor) was heated to the reaction temperature and recirculated through the monolith at a flow rate of 6 mL/min with a concurrent downflow. In addition, the mixture boiled up through the tube forming a bubble column that generated high turbulence in the monolith walls. A condenser above the reactor prevented evaporation losses. After the reaction, the washcoated monolith samples were rinsed with 75 mL of 2-propanol and 100 mL of toluene (for removing residual dioxins), and dried at 100 °C for 24 h. Some reactions were conducted by immersing the washcoated monolith into the reaction mixture under magnetic stirring. These samples are coded as M-used-into.

Both the powder and washcoated monolith samples were reused for four consecutive runs. Due to powder catalyst losses during the subsequent filtration step, the ratio, mg of catalyst/ng I-TEQ, was maintained at approximately 1.29 in the powder catalyst reuse tests (see Table 1). The spent washcoated monolith samples were subjected to three different regeneration methods as follows: (1) calcination and reduction under the conditions specified in section 2.1, (2) reduction (section 2.1) and, (3) reflux washing with 2-propanol at 75 °C for 24 h. This assessment was impossible to perform for the powder catalyst because of the continuous sample loss during the filtration process after the reaction.

2.4 Calculations

183 The fly ash was obtained from the bag filters of an incinerator located in Medellin, Colombia. The
184 characteristics of this sample have been previously reported (Cobo, 2009a). The solid samples were
185 soxhlet extracted with toluene for 48 h. After the reaction, the samples were cleaned in silica,
186 florisil, and alumina columns (Merck, Germany) and analyzed by high-resolution gas
187 chromatography coupled to ion-trap low resolution mass spectrometry–mass spectrometry (HRGC–
188 QITMS/MS) in a CP-3800 GC coupled to a Saturn 2000 ion trap spectrometer (Varian, Walnut
189 Creck, CA, USA), equipped with a DB5-MS low bleed/MS (60 m, 0.25 mm i.d., 0.25 mm film
190 thickness) capillary column (J&W Scientific, CA, USA). All of the solvents employed for the
191 catalytic tests, PCDD/Fs extraction, clean up, and analysis were of Ultimar Grade from
192 Mallinckrodt Baker (MI, USA). The EPA-1613CVS calibration solutions in nonane (Wellington
193 Laboratories, Canada) were employed for instrument calibration and quantification according to
194 EPA 1613 (US EPA, 1994). PCDD/Fs concentrations were calculated using the isotopic dilution
195 method from the Relative Response Factor (RRFs) determined from the CS1 to CS5 injections and
196 area comparison with ^{13}C-labeled internal standard compounds (EPA-1613LCS extraction standard
197 and EPA-1613ISS syringing standard) (Aristizabal, 2008).
198
199 HDC over 2 wt. % Pd/γ-Al_2O_3 washcoated monoliths of toxic compounds (i.e., 7 dioxins and 10
200 furans) was determined by calculating the conversion of the toxic compound from its concentration
201 in the sample before and after the reaction. In addition, the total conversion (TC %) was determined
202 by summing the conversion of all of the toxic compounds before and after the reaction (Eq. 1), and
203 the percent toxicity reduction (TR %) was obtained from the initial and final ng TEQ of each
204 sample (Eq. 2) (Cobo, 2009b).
205
206 $$TC\ (\%) = \frac{\sum_1^{29}[PCDD/PCDF/PCB]_{initial} - \sum_1^{29}[PCDD/PCDF/PCB]_{final}}{\sum_1^{29}[PCDD/PCDF/PCB]_{initial}} \quad \text{(Eq. 1)}$$

$$TR\ (\%) = \frac{(ng\ TEQ)_{initial} - (ng\ TEQ)_{final}}{(ng\ TEQ)_{initial}} \quad \text{(Eq. 2)}$$

3. Results and discussion

3.1 Monolith washcoating

The washcoat weight after each monolith immersion into the starting slurry is shown in Figure 2. Between 6 and 10 wt. % washcoat was obtained after each immersion. The final washcoat was approximately 20 – 30 wt. %, and only three immersions were required to obtain 100 mg of 2 wt. % Pd/Al_2O_3 washcoating. Jiang et al. (2005) studied the effect of pH and solid content on the efficiency of alumina washcoats over ceramic honeycombs. They found that the appropriate solid content in the slurry gel (pH value of 2 to 5) was approximately 30 wt. %, and the first immersion can results in 8–12 wt. % of washcoat, which is similar to that obtained in this study. However, they found that the lower the pH, the higher the loading of the coating (Jinag, 2005). In addition, they reported that the second and third washcoat weights were much lower than the first one, even when the same slurry was used. However, similar weights for each immersion (4 wt. %) were reported by Zamaro et al. (2005a, 2005b) for zeolite washcoating onto cordierite honeycomb from a slurry containing 25 wt. % solids. After each immersion, similar washcoat loadings were obtained in this study with a slurry containing 23 wt. % solids (Figure 2). More concentrated slurries can deliver elevated washcoat weights. The washcoat thickness significantly increases and porous occlusions or mass transfer limitations may be critical, especially inside channels and corners (Zamaro, 2005a, 2005b, Jiang, 2005). Therefore, a 20 – 30 wt. % washcoat weight will produce a stable and thin layer over the monolith.

231 Washcoat weigh losses after the resistant tests are summarized in Table 2. The samples were
232 immersed four times for 1 h each in an ultrasonic bath with either water (Uv-w) or 2-propanol (Uv-
233 2P). The washcoating losses were lower than 11 wt. % in the first immersion under more severe
234 conditions than those used during the catalytic reactions. The total losses were 23.1 and 24.7 wt. %
235 for water and 2-propanol immersions, respectively. The water flow test (Table 2) showed good
236 abrasion resistance. When the monolith was subjected to simulated reaction conditions, a very low
237 washcoating loss (0.2 wt. %) was detected. Jiang et al. (2005) reported total washcoat losses
238 between 23 and 79 wt. % after a 20 min water immersion in an ultrasonic bath. This range was
239 dependent on the apparent viscosity of the slurry where those with a low viscosity exhibited the best
240 stability. Valentini et al. (2001) found a direct relationship between the slurry HNO_3 content and the
241 washcoating loss after 30 min of water immersion in their ultrasonic tests. They reported losses of 0
242 to 95 wt. % when the nitric acid content was increased. According to these results, the dip-coating
243 method employed in the current work produced stable washcoatings on cordierite monoliths.
244 Special conditions including a large number of fine particles stacked on the honeycomb framework
245 contribute to the interaction between the particles and facilitated a convenient filling of the
246 cordierite surface resulting in a firm cohesive interaction between the washcoat and the ceramic
247 honeycomb, and a much higher resistance to mechanical vibration and thermal shock (Jiang, 2005),
248 which was improved with the sol alumina binder (Gonzalez, 2007).
249
250 **3.2 Catalyst characterization**
251
252 The SEM micrograms of the fresh and spent Pd/Al_2O_3 washcoated monoliths are shown in Figure 3.
253 The washcoat consisted of a well-dispersed and homogeneous layer (Figures 3a, 3b and 3f). The
254 film thickness on the fresh monolith is shown in Figure 3a. A thickness of 20 – 30 μm was
255 measured in zone 1 and a maximum thickness (zone 2) was found to be approximately 150 – 200

μm. Similar minimum and maximum thickness have been reported by Zamaro et al. (2005a). In addition, the SEM image of the monolith after a transversal cut shows the washcoat film thickness after each immersion (Figure 3b). The measured thickness of each of the film layer is 30 – 50 μm. The sum of the film layer thickness after each immersion is approximately 150 μm, which corresponds to the maximum thickness measured in the monolith corners (150 – 200 μm). Comparable film thicknesses confirmed similar coat loadings after each immersion, as shown in Figure 2. The thin crack observed in the corners of the washcoat layer was present before (Figure 3b) and after (Figure 3e) the reaction and does not suffer important changes during the reaction. In fact, Villegas et al. (2007) reported the presence of a crack in the corners where the alumina layer is thicker.

The SEM images of the spent washcoated monolith samples after a 5 h reaction are shown in Figures 3c through f. The monolith that was directly placed into the reaction mixture (Figures 3c and 3d) showed clear washcoat erosion. However, the layer on the monolith employed in the bubble loop column (Figures 3e and f) did not suffer appreciable changes. This difference shows a negative effect of the reaction medium on the washcoat layer stability, which can be controlled by the choice of column configuration. The erosion can be accelerated by the high-speed stirring and the different metals and salts present in the fly ash extracts, which create a corrosive environment. Approximately 50 wt. % washcoat loss was detected in the M-used-into monolith, while a small increase in weight (between 3 – 4 mg) was observed in the M-used monolith due to solid deposits, *vide infra*.

Table 3 shows the atomic concentration (at. %) of the elements detected by EDX analysis of the SEM images. The Si from cordierite was observed in all of the monolith samples, and Mg was detected in the M-used-into where the honeycomb exposure was higher. In addition, Na was found

281 in the spent monoliths, which is due to the addition of NaOH to the reaction medium. These sodium
282 deposits have been previously characterized for a powder catalyst (Cobo, 2008b). The detection of
283 Ti and Fe can be attributed to the metals present in the fly ash samples. The palladium crystals
284 observed in Figure 3f were also detected in the EDX analysis where a similar atomic concentration
285 was observed for the M-fresh and M-used samples and a small atomic concentration was observed
286 for the monolith M-used-into due to washcoat layer degradation.
287
288 The Pd particle size distribution of the monolith washcoat before and after the reaction in the bubble
289 loop column (M-fresh and M-used, respectively) is shown in the TEM images in Figure 4. Pd
290 particles, which have similar facets and are 5 nm in diameter, were observed in the fresh and spent
291 samples. More homogeneous and smaller Pd particles were observed in these samples compared to
292 the powder 2% Pd/Al_2O_3 samples (Cobo, 2008b). Therefore, the washcoat preparation method
293 delivered a more homogeneous active phase than that obtained by the incipient wetness
294 impregnation employed for the powder catalyst samples. The variation in the Pd particle size after
295 the HDC reaction was not observed in the washcoated monoliths or powder catalyst samples, which
296 demonstrated the high stability of the active phase on alumina under the reaction conditions. The
297 EDS spectra showed the presence of Pd, Al, and O elements. However, Si was also detected by
298 EDX in the SEM images from the cordierite honeycomb (Table 3). In this analysis, Ca, which is
299 mostly likely present in the fly ash extracts, was found, and Na deposits were observed due to
300 NaOH. A similar Na loading (1.63 %) was found using EDS analysis of the spent powder catalyst
301 samples, which is consistent with previously published report (Cobo, 2008b, 2009b).
302
303 Table 4 shows the metal loading, BET surface area and Pd dispersion for the fresh (PA-Act and M-
304 fresh), after one run (PA-used and M-used), and after four consecutive runs (PA-used4 and M-
305 used4) over 2 wt. $\%Pd/Al_2O_3$ powder and washcoated monolith samples. Pd losses are negligible

after one and four runs confirming the stability of the active phase (Yuan, 2004, Cobo, 2008c). The surface area and Pd dispersion in the fresh powder and monolith catalysts exhibited similar values. The spent catalyst samples also presented a comparable BET surface area reduction, which suggests that the presence of solid deposits affect the textural properties of alumina. However, the monolith samples exhibit high resistance to blockage (Fishwick, 2007), which can be confirmed by the minor reduction of Pd dispersion compared to the powder samples where the active phase occlusion prevents the H_2-Pd interaction during the chemisorption experiment (Cobo, 2008b). No carbon deposits were detected by SEM/EDX or TEM/EDS indicating a very low concentration of this material in the spent samples. Therefore, the BET surface area reduction is most likely due to Na and other metal deposits.

The properties of the 2 wt. % Pd/Al_2O_3 monolith samples regenerated by different methods are shown in Table 4. A slight decrease in the Pd loading was observed, which may be due to the high temperature regeneration applied in methods 1 and 2 and the mechanical strength in method 3 where the catalyst was subjected to solvent reflux for 24 h. In all of the cases, the surface area significantly increased, especially in regeneration method 2. The Pd dispersion also increased after regeneration. The regeneration corresponded to the elimination of inorganic and undetectable carbonaceous residues from the catalyst surface, and the reduction and reduction/calcination treatments appear to be appropriate for this purpose. Solvent washing does not eliminate the more persistent, non-soluble residues, which are most likely removed only at higher temperature.

3.3 Catalytic tests

17 toxic 2,3,7,8-chlorosubstituted PCDD/Fs congeners were quantified during the HDC reaction over the 2 wt. % Pd/Al_2O_3 powder and washcoated monolith catalysts. The results are shown in

331 Figure 5. All of the congeners achieved approximately 100% conversion over the powder samples
332 (Figure 5a). However, only the more chlorinated furans were dechlorinated over the monolith
333 samples (Figure 5b). The dechlorination pathway of the real PCDD/Fs polluted samples has been
334 shown to proceed by a successive process where the more chlorinated congeners react fast to
335 produce the less chlorinated ones and the furans are more reactive than the dioxins (Ukisu, 2004,
336 Yang, 2007, Cobo, 2009b). Therefore, the more toxic 2,3,7,8-TCDD congener required a longer
337 time before it was completely eliminated, and its concentration can increase during the reaction.
338 Almost complete degradation of TCDD after the 5 h reaction was achieved over the powder
339 catalyst. However, TCCD was still present after the 5 h reaction over the monolith (see Table 5).
340
341 In addition, Figure 6 shows the sample toxicity reduction (TR) in each configuration. More
342 important differences were observed at shorter reaction times when the less chlorinated but more
343 toxic congeners were not eliminated. After 1 h, the sample toxicity was reduced by 95% over the
344 powder samples but only reduced by 8% on the monoliths. Nevertheless, the toxicity was reduced
345 by 72% after the 5 h reaction over the monolith samples. Very similar results (70.08% TR) were
346 obtained after the 5 h reaction for monolith samples dipped into the reaction mixture. However,
347 washcoat layer degradation was detected, as shown in Figures 3 c and d. Nijhuis et al. (2003)
348 employed a monolithic stirrer inside the reaction mixture in the selective liquid-phase
349 hydrogenation of alkynes to alkenes with a Pd/silica catalyst. The lower activity of the monoliths
350 compared to the powder catalyst (less than 30 times) was associated with the external mass transfer
351 limitation due to the lower geometrical surface area in the monolith samples. They proposed the use
352 of higher cell-density monoliths (up to 1600 cpsi monoliths) that have a larger geometrical surface
353 area and thinner walls resulting in a more efficient catalyst utilization. Also, Sanchez et al. (2009)
354 tested Pd/Al_2O_3 monoliths for flower oil hydrogenation using 400 cpsi cordierite materials as a

355 monolithic stirrer and observed one third less activity and lower selectivity in the structured catalyst
356 compared to the powder catalysts.
357
358 Tubular reactors employed for hydrogenation reactions have also shown slight lower initial activity
359 but better selectivity than traditional configurations (Marwan, 2004, Vandu, 2005, Fishwick , 2007).
360 Nevertheless, the novel concept of a tubular liquid catalytic reactor operating in a vertical position
361 presents several advantages, because monolithic catalysts provide a large number of parallel
362 capillary channels in which the reaction occurs with good mass-transfer properties and high
363 selectivity. In addition, there is expected to lead to a dramatic decrease (by 1-2 orders of magnitude)
364 in the reactor volume resulting in a significant reduction in the overall plant size (Stankiewicz,
365 2001). The lower catalyst activity can be compensated by improved reusability of the catalyst (no
366 losses when the catalyst is separated from the liquid). This type of reactor is often preferred over a
367 slurry reactor by industry because continuous operation is cheaper and simpler (Edvinsson, 1998,
368 Nijhuis, 2003). No important differences between the M-used-into and M-used samples were
369 observed, which indicated that reactants can reach the catalyst over the monolith walls to the same
370 extent. However, the bubble loop column appears to be more capable of preserving the washcoat
371 stability for further use. Therefore, this configuration was employed in subsequent tests.
372
373 Figure 7a shows the reactivity of the spent samples for PCDD/Fs HDC in the slurry reactor and in
374 the bubble loop column. The powder catalyst amount decreased after each successive reuse in the
375 filtration step. Therefore, the PCDD/Fs initial concentrations diminished to maintain a constant ratio
376 of 1.29 for the mg of catalyst/ng I-TEQ (Table 1). However, the activity of these samples
377 significantly decreased from 98.24 to 6.43% TR after 4 runs. The fast decline in reactivity has been
378 attributed to several issues including the porous and active site occlusion by carbonaceous and
379 sodium deposits (Cobo, 2008b, 2009b). By contrast, the monolith catalyst maintained their

reactivity of approximately 43% for several runs, and there was no catalyst loss after the reaction. In fact, the spent monoliths were slightly heavier than the fresh ones. Despite the particle size of the powder catalyst (37 µm), the washcoat thickness (20 – 30 µm), and the surface area loss after use being similar (Table 4), the reactivity of the monolith catalyst did not vary significantly, because the homogeneity and deposition of the washcoat layer results in the active sites being more accessible for the reactants reducing the negative impact of the deposits. In addition, the nature of these deposits is mostly carbonaceous for the powder catalyst and inorganic for the monoliths, which may alter the deactivation mechanism in different ways. The lower metal dispersion reduction of the monolith samples suggests that the active sites are more available in this arrangement (Table 4).

Figure 7b shows the effect of regeneration tests on monolith reactivity. Approximately 43% TR was obtained without regeneration, and this value was increased to approximately 65% with both regeneration methods. Among the tested methods, washing with solvent under reflux conditions (method 3) has the advantage of being economic and practical because it requires less energy and offers the potential for *in-situ* regeneration with fresh solvent. Concibido et al. (2007) washed the Pd/C deactivated catalyst employed in the tetrachloroethylene HDC by stirring it in water or MeOH for 24 h. The catalyst recovered its initial activity, which suggests that the deactivation was primarily due to the adsorption of the reaction products on the catalyst. However, the combustion of more persistent deposits adsorbed on the catalyst and the subsequent reduction of the active metal (method 1) can deliver improved recovery of the surface area and Pd dispersion (Table 4). This regeneration method has been applied successfully to Pd catalysts for the hydrogenation reaction (Liu, 2005), and it is appropriate for catalysts regenerated several times by a washing process. In addition, Ordoñez et al. (2007) tested three regeneration methods for the reactivation of the Pd/Al_2O_3 catalyst employed for tetrachloroethylene HDC including calcination, reduction, and leaching with ammonia followed by calcination and reduction. The last method was the best for

405 catalyst reactivation. In addition, the regenerated catalyst was even less prone to deactivation than
406 the fresh catalyst, which showed that the combination of the washing and calcination/reduction
407 methods is the best procedure for catalyst reactivation. Furthermore, it has been shown that
408 preemptive regeneration processes can extend the period of stable activity (Simson, 2011).
409
410 **4. Conclusions**
411
412 A stable and homogeneous 2 wt. % Pd/Al_2O_3 washcoat layer is deposited over cordierite monoliths
413 by dip coating in a neutral 23 wt. % solids slurry followed by microwave drying. In spite of both
414 monolith batch and bubble loop column reactors have similar catalytic activity (c.a. 70 % TR), the
415 tubular configuration maintains the washcoat stability and the monolith batch reactor causes layer
416 erosion. The monoliths exhibit an approximately 30 % lower activity than the powder samples after
417 one run, but the powder deactivates easily and its reuse is limited by sample loss during the
418 filtration process. Although the BET surface area decreases in the spent samples of the powder and
419 monolith catalysts, the catalytic activity of the monoliths in the bubble loop column remains
420 constant (i.e., approximately 43 % TR after 2, 3, and 4 runs), which may be due to the different
421 nature of the solid blockage and better distribution of the solid deposits over the thin layer of the
422 Pd/Al_2O_3 washcoated monolith.
423
424 In addition, the catalytic activity of the monolith samples increased up to 63 % TR after
425 oxidation/reduction, reduction, and washing treatments. The low energy consumption of the
426 washing treatment is highly attractive for the *in-situ* recovery of catalytic activity. However, the
427 more stable solid deposits on the catalyst surface must be eliminated by high temperature
428 treatments.
429

Acknowledgments

The authors are grateful to the University of Antioquia, the University of La Sabana, and the University of Alicante for financial support of this work. We are also grateful to Professor Consuelo Montes de Correa for her tutoring and guidance (RIP), and Carlos Andrés González and Alexander Quintero for their collaboration and support.

References

Albers, R.E., Nyström, M., Siverström, M., Sellin, A., Dellve, A.-C., Andersson, U., Herrmann, W., Berglin, T.H. 2001. Development of a monolith-based process for H_2O_2 production: From idea to large-scale implementation. Catalysis Today 69, 247-252.

Albers. R.E. 2005. Characterization of the performance of an industrial monolith reactor by accurate mapping of temperature differences. Catal. Today 105, 391-395.

Aristizábal, B., Cobo, M., Hoyos, A., Montes de Correa, C., Abalos, M., Martínez, K., Abad, E., Rivera, J. 2008. Baseline levels of dioxin and furan emissions from waste thermal treatment in Colombia. Chemosphere 73, S171-S175.

Avila, P., Montes, M., Miro, E. 2005. Monolithic reactors for environmental applications. A review on preparation technologies. Chemical Engineering Journal 109, 11–36

Concibido, N.C., Okuda, T., Nishijima, W., Okada, M. 2007. Deactivation and reactivation of Pd/C catalyst used in repeated batch hydrodechlorination of PCE. Applied Catalysis B: Environmental 71, 64–69.

Cobo, M., Quintero, A., Montes, C. 2008a. Liquid phase dioxin hydrodechlorination over Pd/γ–Al_2O_3. Catalysis Today 133–135, 509–519.

454 Cobo, M., Conesa, J.A., Montes de Correa, C. 2008b. The effect of NaOH on the liquid-phase
455 hydrodechlorination of dioxins over Pd/γ-Al_2O_3. The Journal of Physical Chemistry A 112,
456 8715–8722.
457 Cobo, M., Gálvez, A., Conesa, J.A., Montes de Correa, C. 2009a. Characterization of fly ash from a
458 hazardous waste incinerator in Medellin, Colombia. Journal of Hazardous Materials 168, 1223–
459 1232.
460 Cobo, M., Conesa, J.A., Montes de Correa, C. 2009b. Effect of the reducing agent on the
461 hydrodechlorination of dioxins over 2 wt.% Pd/γ-Al_2O_3. Applied Catalysis B: Environmental
462 92, 367-376.
463 Cobo, M., González, C.A., Sánchez, E.G., Montes, C. 2011. Catalytic hydrodechlorination of
464 trichloroethylene with 2-propanol over Pd/Al_2O_3. Catalysis Today 172, 78-83.
465 Cybulski, A., Stankiewicz, A., Albers, R.K., Moulijn, J.A. 1999. Monolithic Reactors for Fine
466 Chemicals Industries: A Comparative Analysis of a Monolithic Reactor and a Mechanically
467 Agitated Slurry Reactor. Chemical Engineering Science 54, 2351-2358.
468 Delattre, C., Vijayalakshmi, M.A. 2009. Monolith enzymatic microreactor at the frontier of
469 glycomic toward a new route for the production of bioactive oligosaccharides. Journal of
470 Molecular Catalysis B: Enzymatic 60, 97-105.
471 Ebrahimi, S., Kleerebezem, R., Kreutzer, M.T., Kapteijn, F., Moulijn, J.A., Heijnen, J.J., Van
472 Loosdrecht, M.C.M. 2006. Potential application of monolith packed columns as bioreactors,
473 control of biofilm formation. Biotechnology and Bioengineering 93, 238-245.
474 Eisenbeis, C., Guettel, R., Kunz, U., Turek, T. 2009. Monolith loop reactor for hydrogenation of
475 glucose. Catalysis Today 147S, S342–S346
476 Edvinsson, R.K., Houterman, M.J.J., Vergunst, T., Grolman, E., Moulijn, J.A. 1998. Novel
477 Monolithic Stirred Reactor. Reactors, Kinetics, and Catalysis 44, 2459-2464.

478 Fishwick, R.P., Natividad, R., Kulkarni, R. McGuire, P.A., Wood, J., Winterbottom, J. M., Stitt, E.
479 H. 2007. Selective hydrogenation reactions: A comparative study of monolith CDC, stirred
480 tank and trickle bed reactors. Catalysis Today 128, 108-114.
481 Gómez-Quero, S., Cárdenas-Lizana, F., Keane, M.A. Liquid phase catalytic hydrodechlorination of
482 2,4-dichlorophenol over Pd/Al_2O_3: Batch vs. continuous operation. Chemical Engineering
483 Journal 166, 1044-1051.
484 González, C.A., Ardila, A.N., De Correa, C.M. , Martínez, M.A., Fuentes-Zurita, G. 2007. Pd/TiO_2
485 washcoated cordierite minimonoliths for hydrodechlorination of light organochlorinated
486 compounds. Industrial and Engineering Chemistry Research 46, 7961-7969.
487 Heiszwolf, J.J., Kreutzer, M.T., van den Eijnden, M.G., Kapteijn, F., Moulijn, J.A. 2001. Gas–
488 liquid mass transfer of aqueous Taylor flow in monoliths. Catalysis Today 69, 51–55.
489 Huang, X., Yuan D. 2012. Recent developments of extraction and micro-extraction technologies
490 with porous monoliths. Critical Reviews in Analytical Chemistry 42, 38-49.
491 Jiang, P., Lua, G., Guoa, Y., Guoa, Y., Zhanga, S., Wang, X. 2005. Preparation and properties of a
492 γ-Al_2O_3 washcoat deposited on a ceramic honeycomb. Surface & Coatings Technology 190,
493 314–320.
494 Keane. 2011. Supported transition metal catalysts for hydrodechlorination reactions. ChemCatChem
495 3, 800-821.
496 Kulkarni, R., Natividad, R., Wood, J., Stitt, E.H., Winterbottom, J.M. 2005. A comparative study of
497 residence time distribution and selectivity in a monolith CDC reactor and a trickle bed reactor.
498 Catalysis Today 105, 455–463.
499 Liu, R.J., Crozier, P.A.. Smith, C.M., Hucul, D.A. Blackson, J., Salait, G. 2005. Metal sintering
500 mechanisms and regeneration of palladium/alumina hydrogenation catalysts. Applied Catalysis
501 A: General 282, 111–121.

Marwan, H., Winterbottom, J.M.. 2004. The selective hydrogenation of butyne-1,4-diol by supported palladiums: a comparative study on slurry, fixed bed, and monolith downflow bubble column reactors. Catalysis Today 97, 325–330.

Morales, M.R., Barbero, B.P., Cadús, L.E. 2011. MnCu catalyst deposited on metallic monoliths for total oxidation of volatile organic compounds. Catalysis Letters 141, 1598-1607.

Moulijn, J.A., Kreutzer, M.T., Nijhuis, T.A., Kapteijn, F. 2011. Chapter 5 – Monolithic Catalysts and Reactors: High Precision with Low Energy Consumption. Advances in Catalysis. 54, 249–327.

Nijhuis, T.A., Kreutzer, M.T., Romijn, A.C.J., Kapteijn, F., Moulijn, J.A. 2001. Monolithic catalysts as more efficient three-phase reactors. Catalysis Today 66, 157–165.

Nijhuis, T.A., van Koten, G., Moulijn, J.A. 2003a. Optimized palladium catalyst systems for the selective liquid-phase hydrogenation of functionalyzed alkynes. Applied Catalysis A: General 238, 259–271.

Nijhuis, T.A., Dautzenbergb, F.M., Moulijn, J.A. 2003b. Modeling of monolithic and trickle-bedreactors for the hydrogenation of styrene. Chemical Engineering Science 58 (2003) 1113 – 1124.

Ordóñez, S., Díaz, E., Díez, F.V., Sastre, H. 2007. Regeneration of Pd/Al_2O_3 catalysts used for tetrachloroethylene hydrodechlorination. Reaction & Kinetic Catalysis Letters 90, 101-106.

Sánchez M, J.F., González Bello, O.J., Montes, M., Tonetto, G.M., Damiani, D.E. 2009. Pd/Al_2O_3-cordierite and Pd/ Al_2O_3-Fecralloy monolithic catalysts for the hydrogenation of sunflower oil. Catalysis Communications 10, 1446-1449.

Simson, A., Farrauto, R., Castaldi, M. 2011. Steam reforming of ethanol/gasoline mixtures: Deactivation, regeneration and stable performance. Applied Catalysis B: Environmental 106, 295-303.

526 Smiths, H.A., Stankiewicz, A., Glasz, W. C., Fogl, T.H.A., Moulijn J.A.. 1996. Selective three-
527 phase hydrogenation of unsaturated hydrocarbons in a monolithic reactor. Chemical
528 Engineering Science 51, 3019-3025.
529 Stankiewicz, Process intensification in in-line monolithic reactor. Chemical Engineering Science
530 56, 359-364.
531 Tsoligkas, A.N., Simmons, M.J.H., Wood, J. 2007. Influence of orientation upon the
532 hydrodynamics of gas–liquid flow for square channels in monolith supports. Chemical
533 Engineering Science 62, 4365 – 4378.
534 US EPA. 1994. Method 1613: Tetra-through Octa-chlorinated Dioxins and Furans by isotopic
535 dilution HRGC/HRMS, Washington (USA).
536 Ukisu, Y., Miyadera, T. 2004. Dechlorination of dioxins with supported palladium catalysts in 2-
537 propanol solution. Applied Catalysis A: General 271, 165-170.
538 Valentini, M., Groppi, G., Cristiani, C., Levi, M., Tronconi, E., Forzatti, P. 2001. Catalysis Today
539 69, 307-314.
540 Vandu, C.O., Ellenberger, J., Krishna, R. 2005. Hydrodynamics and mass transfer in an upflow
541 monolith loop reactor. Chemical Engineering and Processing 44, 363–374.
542 Villegas, L., Masset, F., Guilhaume, N. 2007. Wet impregnation of alumina-washcoated monoliths:
543 Effect of the drying procedure on Ni distribution and on autothermal reforming activity.
544 Applied Catalysis A: General 320, 43–55.
545 Xiaoding, X., Vonk, H., van de Riet, A.C.J.M., Cybulski, A., Stankiewicz, A., Moulijn, J.A. 1996.
546 Monolithic catalysts for selective hydrogenation of benzaldehyde. Catalysis Today 30, 91-97.
547 Yang, Z., Xia, C., Zhang, Q. Chen, J., Liang, X. 2007. Catalytic detoxification of polychlorinated
548 dibenzo-p-dioxins and polychlorinated dibenzofurans in fly ash. Waste Management 27, 588–
549 592.

Yu, Y.H., Pan, Y.T., Wu, Y.T., Lasek, J., Wu, J.C.S. 2011. Photocatalytic NO reduction with C_3H_8 using a monolith photoreactor. Catalysis Today 174, 141-147.

Yuan, G., Keane, M. 2004. Liquid phase hydrodechlorination of chlorophenols over Pd/C and Pd/Al_2O_3: a consideration of HCl/catalyst interactions and solution pH effects. Applied Catalysis B: Environmental 52, 301-314.

Zamaro, J.M., Ulla, M.A., Miro, E.E. 2005a. The effect of different slurry compositions and solvents upon the properties of ZSM5-washcoated cordierite honeycombs for the SCR of NOx with methane. Catalysis Today 107–108, 86–93.

Zamaro, J.M., Ulla, M.A., Miro, E.E. 2005b. Zeolite washcoating onto cordierite honeycomb reactors for environmental applications. Chemical Engineering Journal 106, 25–33.

560

561 **Figure captions**

562

563 **Figure 1** Schematic representation of the monolithic bubble loop column setup.

564 **Figure 2** Weight of the monolith after each immersion into the catalytic slurry.

565 **Figure 3** SEM images the of 2 wt. % Pd/Al_2O_3 washcoated monoliths: top view (a) and transversal
566 cut (b) of fresh monoliths; top view of monolith immersed into the reaction mixture (M-used-into)
567 after the 5 h reaction (c and d); top view (e) and internal walls (f) of monolith employed in the
568 tubular reactor (M-used) after the 5 h reaction.

569 **Figure 4** TEM images and EDS spectra of (a) fresh and (b) spent 2 wt. % Pd/Al_2O_3 washcoated
570 monoliths, and (c) the particle size distribution of Pd.

571 **Figure 5** Conversion of 2,3,7,8-chlorosubstituted PCDDs and PCDFs as a function of time in HDC
572 over 2 wt. % Pd/Al_2O_3 for the (a) powder and (b) monolith samples. Reaction conditions: 77.35 ng
573 I-TEQ, 100 mg of catalyst, 30 mg NaOH, 20 mL 2-propanol, 75ºC.

574 **Figure 6** PCDD/Fs toxicity reduction (TR) as a function of time during HDC over the 2 wt. %
575 Pd/Al_2O_3 powder and monolith samples. Reaction conditions: 77.35 ng I-TEQ, 100 mg of catalyst,
576 30 mg NaOH, 20 mL 2-propanol, 75ºC.

577 **Figure 7** (a) Reactivity of 2 wt. % Pd/Al_2O_3 powder (PA) and monolith (Monolith) catalysts for
578 PCDD/Fs HDC and (b) reactivity of monolith samples after regeneration. Reaction conditions: 30
579 mg NaOH, 20 mL 2-propanol, 75ºC, 5 h-reaction.

580

581 **Table 1** Catalyst/dioxin ratio in consecutive runs of the dioxin HDC in the slurry reactor.

Run	Catalyst amount (mg)	Initial PCDD/Fs (ng I-TEQ)	**R**atio
1	139.3	108.23	1.29
2	113.3	88.05	1.29
3	56.9	44.25	1.29
4	18.5	14.42	1.28

582

583

584 **Table 2** Percentage (%) washcoat weight losses after water (uv-w) and 2-propanol (uv-2P)

585 ultrasonic vibration, water flow (wf), and simulated reaction conditions (rc).

Uv Immersion	Uv-w[a]	Uv-2P[b]	wf[c]	rc[d]
1	11.0	9.1	1.6	0.2
2	9.6	10.0	--	--
3	4.5	7.9	--	--
4	9.5	7.3	--	--
Total loss	23.1	24.7	1.6	0.2

586 [a]Ultrasonic vibration in water for 1 h each

587 [b]Ultrasonic vibration in 2-propanol for 1 h each

588 [c]30 mL/s water flow for 30 min

589 [d]Simulated reaction conditions in 2-propanol for 6 h at 75 °C

590

591 **Table 3** Atomic concentration (at. %) of the elements detected by EDX in the SEM images.

Catalyst	SEM Image	Element							
		Al	Si	Pd	O	Na	Mg	Ti	Fe
M-fresh	*a*	30.72	1.29	0.48	67.51	N.D.	N.D.	N.D.	N.D.
M-fresh	*b*	31.44	1.49	0.53	66.53	N.D.	N.D.	N.D.	N.D.
M-used-into	*c*	14.89	12.44	0.13	66.60	0.70	4.86	0.18	0.21
M-used-into	*d*	14.44	11.94	0.09	67.71	0.63	4.90	0.10	0.20
M-used	*f*	30.41	0.99	0.47	66.59	1.54	N.D.	N.D.	N.D.
M-used	*g*	28.50	1.02	0.37	68.73	1.39	N.D.	N.D.	N.D.

592 N.D.: Not detected.

593

594 **Table 4** Pd loading, BET surface area and metal dispersion of fresh and spent 2 wt. % Pd/Al_2O_3

595 catalyst samples.

Catalyst sample	Pd loading (%)	BET surface area (m^2/g)	Pd dispersion (%)
	Powder catalyst		
PA-fresh	2.2	76.8	17.4
PA- used	2.4	43.2	1.7
PA-used4	2.2	11.5	0.6
	Washcoated monolith samples		
M-fresh	1.9	70.6	17.1
M-used	2.0	42.9	6.7
M-used4	1.8	14.2	2.1
M-R1	1.8	62.9	14.7
M-R2	1.8	73.5	10.5
M-R3	1.7	54.1	12.0

596 M: Monolith catalyst, PA: powder catalyst, R1: catalyst regeneration by calcination and reduction,

597 R2: catalyst regeneration by reduction, and R3: catalyst regeneration by 2-propanol washing.

598

599 **Table 5** Evolution of 2,3,7,8-TCDD (pg) as a function of time in the HDC reaction with 2 wt. %

600 Pd/Al_2O_3 in the powder and washcoated on monolith catalysts.

Reaction time (h)	Powder catalyst	Monolith catalyst
0	1499.19	1646.57
1	1245.79	2484.23
3	216.96	3089.85
5	21.22	3429.94

601

Figure 1

Click here to download Figure: Fig 1.pdf

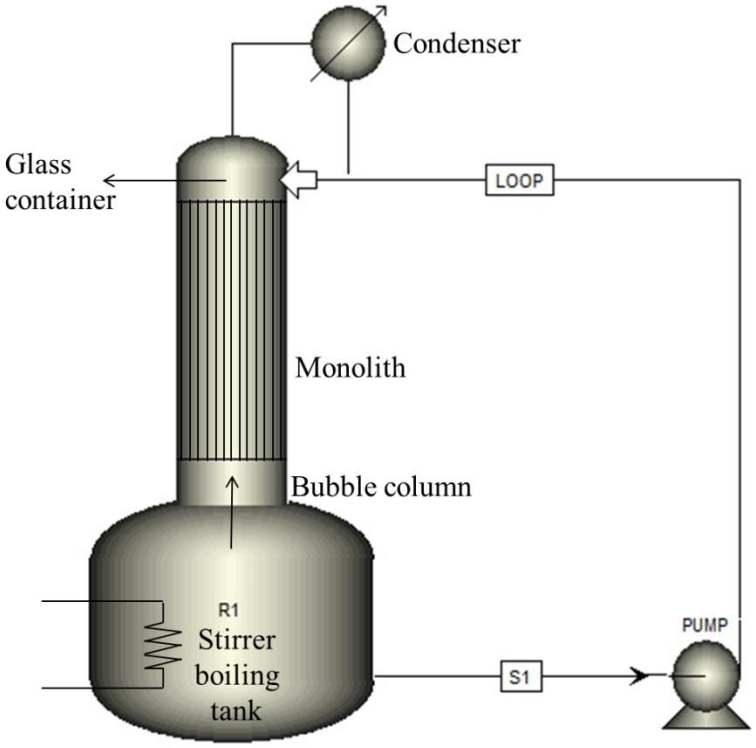

Figure 2

Click here to download Figure: Fig 2.pdf

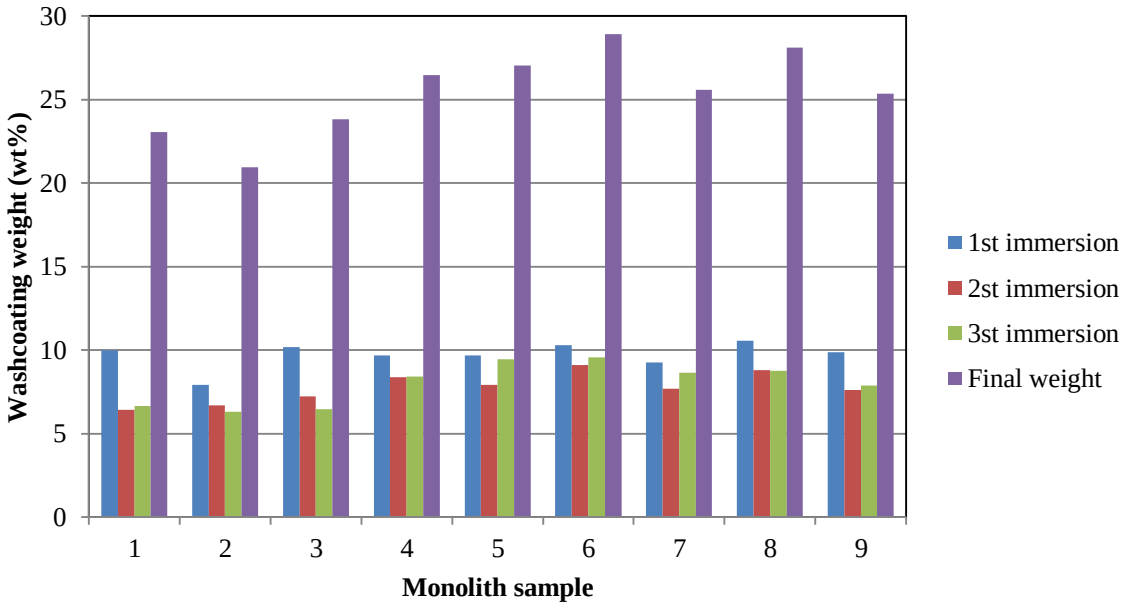

Figure 3

Click here to download Figure: Fig 3.pdf

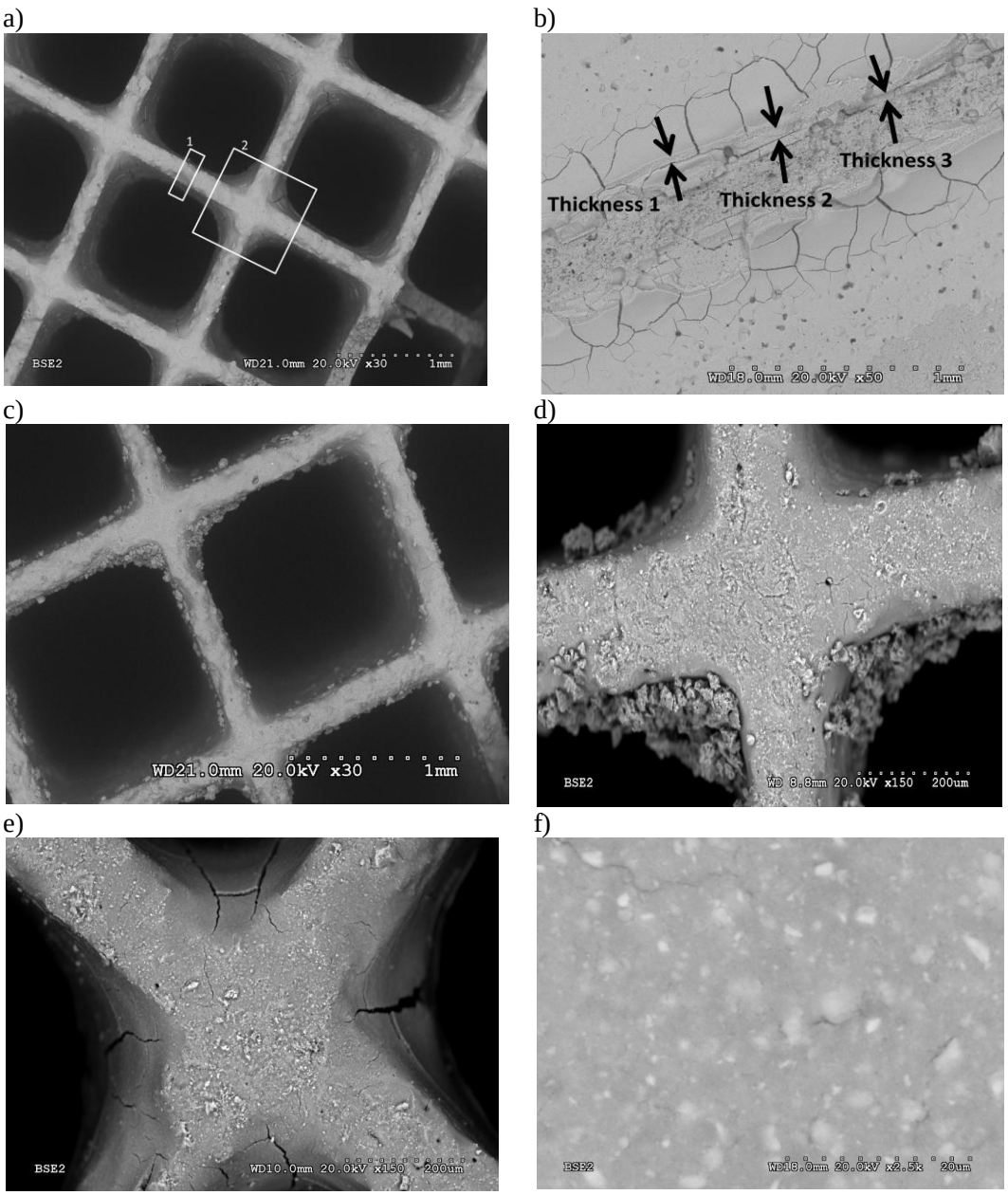

Figure 4

Click here to download Figure: Fig 4.pdf

a)

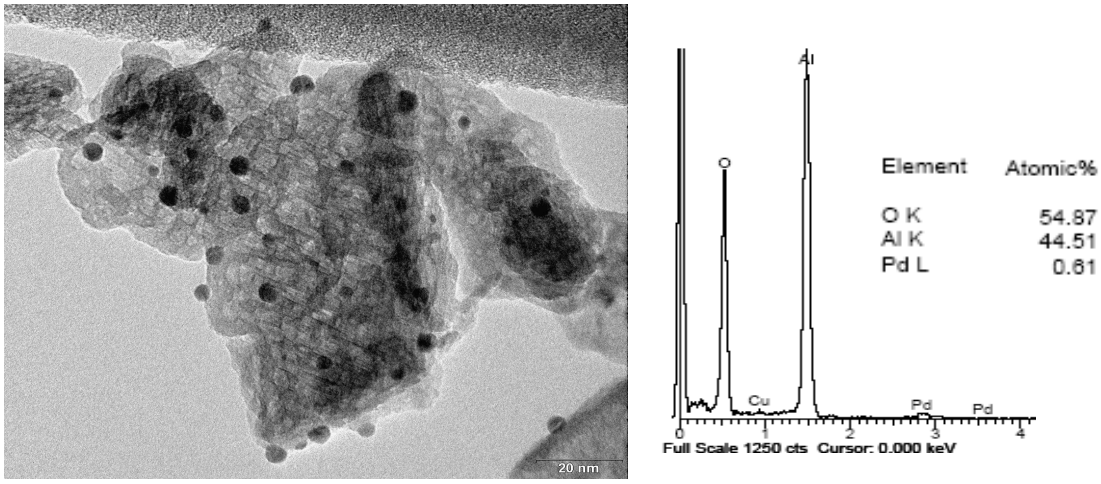

b)

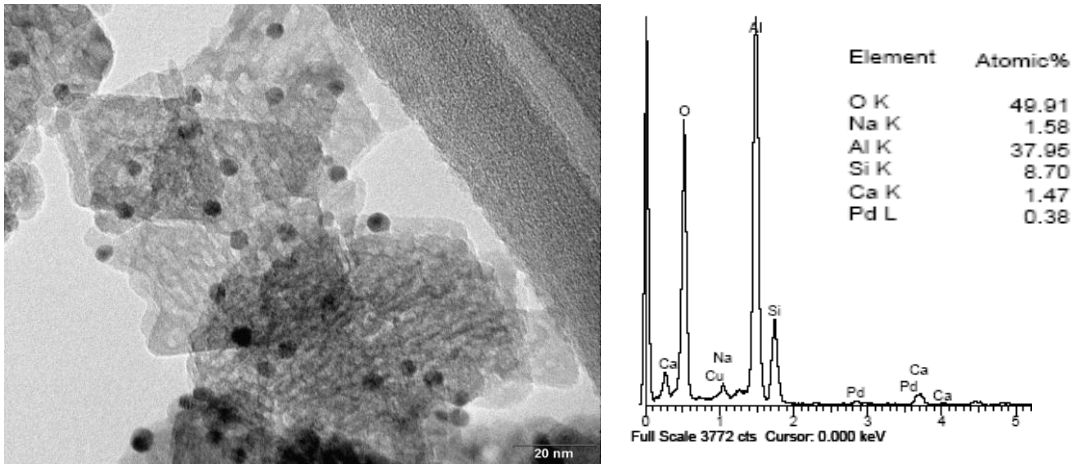

c)

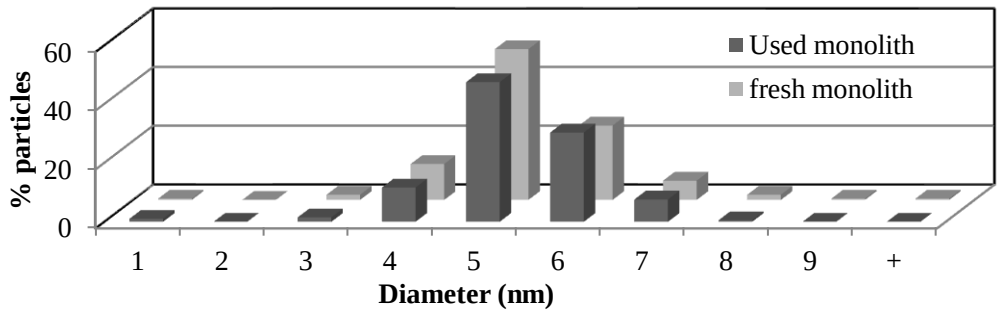

Figure 5

Click here to download Figure: Fig 5.pdf

a)

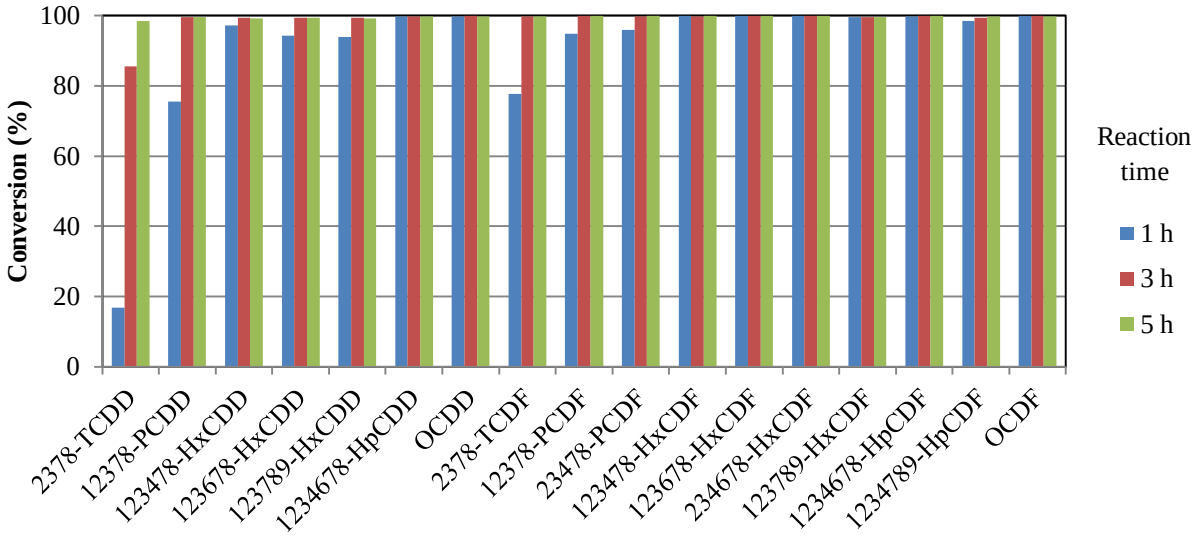

b)

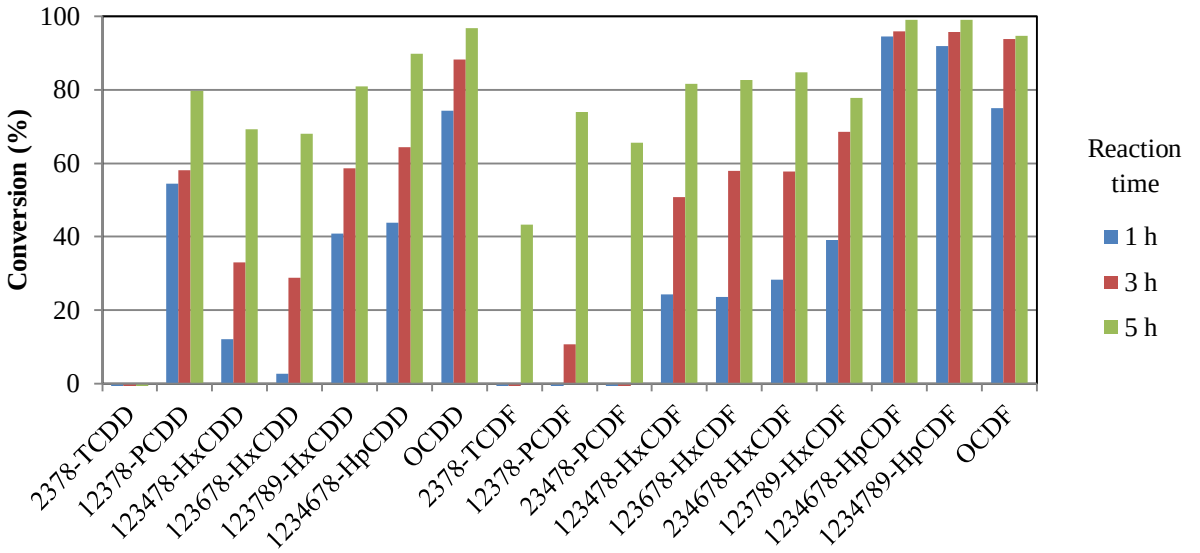

Figure 6

Click here to download Figure: Fig 6.pdf

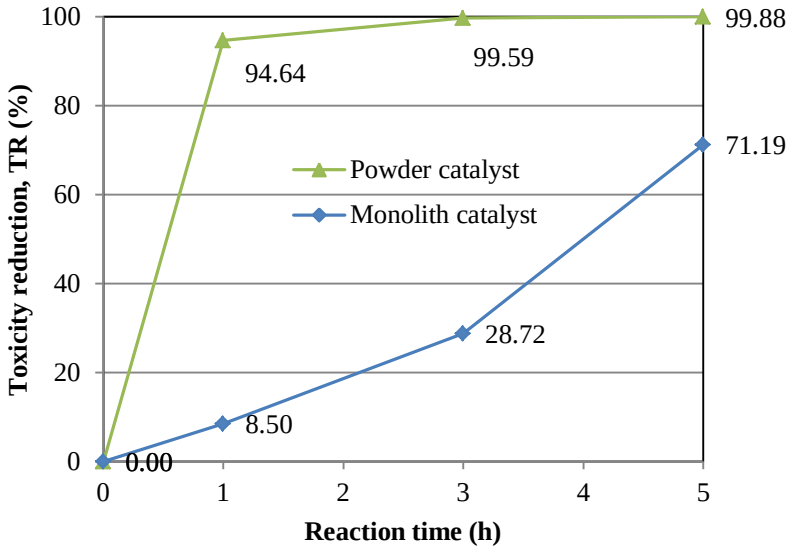

Figure 7

Click here to download Figure: Fig 7.pdf

(a)

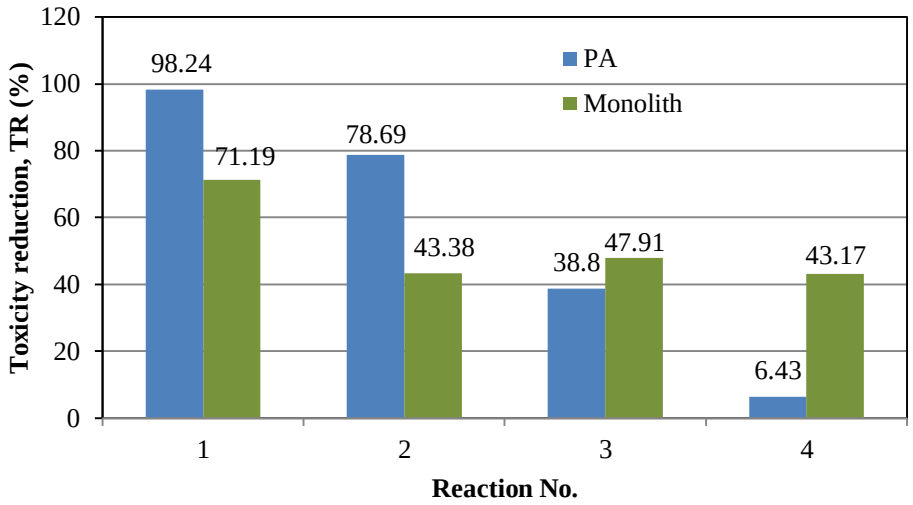

(b)